



**HAL**  
open science

## Diagnosis of induction machines by parameter estimation

Smail Bachir, Slim Tnani, Gérard Champenois, Jean-Claude Trigeassou

► **To cite this version:**

Smail Bachir, Slim Tnani, Gérard Champenois, Jean-Claude Trigeassou. Diagnosis of induction machines by parameter estimation. ISTE Ltd and John Wiley & Sons Inc. Control Methods for Electrical Machines, ISTE Ltd and John Wiley & Sons Inc, pp.249-273, 2009, 9781848210936. 10.1002/9780470611760.ch8 . hal-00782892

**HAL Id: hal-00782892**

**<https://hal.science/hal-00782892>**

Submitted on 30 Jan 2013

**HAL** is a multi-disciplinary open access archive for the deposit and dissemination of scientific research documents, whether they are published or not. The documents may come from teaching and research institutions in France or abroad, or from public or private research centers.

L'archive ouverte pluridisciplinaire **HAL**, est destinée au dépôt et à la diffusion de documents scientifiques de niveau recherche, publiés ou non, émanant des établissements d'enseignement et de recherche français ou étrangers, des laboratoires publics ou privés.

## Chapitre 1

# Diagnosis of induction machines by parameter estimation

**Smail Bachir<sup>1</sup>, Slim Tnani<sup>2</sup>, Gérard Champenois<sup>2</sup> and Jean-Claude Trigeassou<sup>2</sup>**

<sup>1</sup>University of Poitiers, XLIM Laboratory, SIC department  
Bât. SP2MI, Téléport 2, Bvd Marie et Pierre Curie, 86962 Futuroscope Chasseneuil  
Cedex, France

URL : <http://www.sic.sp2mi.univ-poitiers.fr/>  
Corresponding author : [smail.bachir@univ-poitiers.fr](mailto:smail.bachir@univ-poitiers.fr)

<sup>2</sup>University of Poitiers, LAII Laboratory  
Avenue du Recteur Pineau  
86022 Poitiers cedex, France

## Chapter 1

# Diagnosis of Induction Machines by Parameter Estimation

### 1.1. Introduction

In a simple technology, the asynchronous machine or induction motor, is intensively used in most electrical drives, especially for constant speed applications such as ventilation and pumping. All progress of power electronics associated with modern control allowed to consider efficient variable speed applications that previously was reserved for DC engine and more recently in synchronous drives. An illustration is the three generations of high-speed trains used in France (TGV): the first one (south-east), commercialized in 1981 is equipped with a DC motor, the second (south-west in 1989) by synchronous motors and the latest, Eurostar in 1994 with asynchronous motors. Thus, in view of all these economic issues, a general reflection has been initiated for safety operating oriented to the diagnosis of induction machines. The aim of this monitoring is to detect the electrical and mechanical faults in the stator and the rotor of induction motors.

The diagnosis of induction machine under fixed speed has been intensively studied in the literature contrary to the applications under variable speed. Indeed, the signals being highly non-stationary, approaches based on conventional Fourier analysis of currents lines [ABE 99, INN 94, FIL 94], stator voltages and electromagnetic torque [MAK 97, MAL 99] proving inadequate. A considerable effort has been undertaken in the last decade in parameters identification of continuous models [TRI 88, MEN 99,

---

Chapter written by Smail BACHIR, Slim TNANI, Gérard CHAMPENOIS and Jean Claude TRIGEASSOU.

MOR 99b]. Requiring rich excitation of machine modes, parameter estimation is well suited for diagnosis in variable speed drive. Thus, algorithms development dedicated to a realistic physical parameters estimation [MOR 99b, TRI 99], taking into account a prior knowledge of the machine, has allowed promising advancing in diagnosis of induction machines. This approach based on parameter identification of a model, one of the most important goals, is the development of mathematical models really representative of default operations.

In faulty case, the induction machine present in addition to a conventional dynamic behavior, a default one [BAC 01a, BAC 01b, BAC 06]. In modeling for diagnosis, it is essential to consider two modes: a "common" and a "differential" mode. The common mode describes the dynamic model of the induction machine and translates the healthy model of the machine. The differential mode gives information on a defect. The parameters of this mode should be essentially sensitive to the faults. This situation is useful to the effective detection and localization. Indeed, a change in temperature or magnetic state is reflected by a change in the state of common-mode parametric model, but does not affect differential mode [SCH 99, BAC 01a]. This diagnosis method required to carry out a global parameter estimation of the two model modes. Thus, the electrical parameters of common-mode indicate the dynamic state of the machine (constant rotor time, magnetizing inductance, etc.). Parameters of differential mode explain the default information and the monitoring of these parameters allows detection and localization of the imbalance.

In this chapter, we study in the first part two faulty models which takes into account the effects of inter turn faults resulting in the shorting of one or more circuits of stator phase winding and broken rotor bars. To take into account a simultaneous stator and rotor faults, a global faulty model of the machine will be presented. The corresponding diagnosis procedure based on parameter estimation of the stator and rotor faulty model and more experimental results are presented on the second part.

## **1.2. Induction motor model for faults detection**

For diagnosis of induction motors, it is useless to consider an unbalanced two axis Park's model [MOR 99b, SCH 99]. The deviation of their electrical parameters is certainly an indication of a new situation in the machine, but this evolution can be due to heating or an eventual change in magnetic state of the motor [MOR 99b]. On the other hand, it is very difficult to distinguish stator faults from rotor ones. The use of Fast Fourier's analysis of identification residuals is an original method to localize a fault, but estimation of electrical parameters is unable to obtain the fault level.

A good solution is the introduction of an additional model to explain the faults [BAC 02][BAC 01b]. The parameters of this differential model allow detection and localization of the faulty windings.

### 1.2.1. Stator faults modeling in induction motor

In order to take into account the presence of inter turns short circuit windings in the stator of an induction motor, an original solution is to consider a new winding dedicated to the stator fault [SCH 99]. The new model is composed of an additional shorted winding in three phases axis. Figure (1.1) shows a three phases, 2-poles, induction machine in case of short circuit winding. This faults induces in stator a new windings  $B_{cc}$  short circuited and localized by the angle  $\theta_{cc}$ .

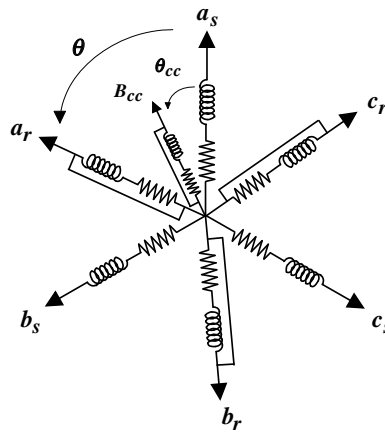


Figure 1.1. Motor windings with a short circuit

Two parameters are introduced to define the stator faults

- The localization parameter  $\theta_{cc}$  which is a real angle between the short circuit inter turn stator winding and the first stator phase axis (phase  $a$ ). This parameter allows the localization of the faulty winding and can take only three values  $0$ ,  $\frac{2\pi}{3}$  or  $\frac{4\pi}{3}$ , corresponding respectively to a short circuit on the stator phases  $a$ ,  $b$  or  $c$ .

- The detection parameter  $\eta_{cc}$  equal to the ratio between the number of inter turn short circuit windings and the total number of inter turns in one healthy phase. This parameter allows to quantify the unbalance and to obtain the number of inter turns in short circuit.

#### 1.2.1.1. Short circuit model

On three-phase windings, we define the vector of stator voltages and currents, respectively  $\underline{u}_s$  and  $\underline{i}_s$ , and the vector of rotor currents  $\underline{i}_r$  :

$$\underline{u}_s = \begin{pmatrix} u_a \\ u_b \\ u_c \end{pmatrix} \quad \underline{i}_s = \begin{pmatrix} i_{s_a} \\ i_{s_b} \\ i_{s_c} \end{pmatrix} \quad \underline{i}_r = \begin{pmatrix} i_{r_a} \\ i_{r_b} \\ i_{r_c} \end{pmatrix}$$

In general case, as a result of a short circuit it follows vibrations and torque oscillations synonymous with the presence of new components in the electromagnetic torque and therefore in the stator currents [MOR 99b, BAC 06]. Indeed, a short-circuiting of turns is at origin of a new stator winding with a strong current and consequently, an additional magnetic field in the machine. For example, consider the case of a healthy machine with  $p$  poles-pairs. When the three phases currents system with a pulsation of  $\omega_s = 2\pi f_s$  flows through the stator windings, three stationary magnetic excitations directed along the axis of each phase will be created. It is the sum of these excitations which creates a rotating field in the airgap at the pulsation of  $\Omega_s = \frac{\omega_s}{p}$  according to the original winding.

When a stator fault occurs, an additional shorted circuit winding  $B_{cc}$  appears in the stator. This winding creates a stationary magnetic field  $H_{cc}$  at the pulsation  $\Omega_s$  oriented according to the faulty winding. In this case, a strong current, noted  $i_{cc}$ , flows through the short circuit winding  $B_{cc}$ . It is the interaction of  $H_{cc}$  with a rotating motor field which introduces a torque ripples and a new electromagnetic forces. With assumption of system linearity, this situation is equivalent to a superposition of "common" operating mode producing a rotating field and a "differential" one producing a faulty field. Voltage and flux equations for faulty model of induction machine can be written as :

$$\underline{u}_s = [R_s] \underline{i}_s + \frac{d}{dt} \underline{\phi}_s \quad [1.1]$$

$$\underline{0} = [R_r] \underline{i}_r + \frac{d}{dt} \underline{\phi}_r \quad [1.2]$$

$$0 = R_{cc} i_{cc} + \frac{d}{dt} \phi_{cc} \quad [1.3]$$

$$\underline{\phi}_s = [L_s] \underline{i}_s + [M_{sr}] \underline{i}_r + [M_{scc}] i_{cc} \quad [1.4]$$

$$\underline{\phi}_r = [M_{rs}] \underline{i}_s + [L_r] \underline{i}_r + [M_{rcc}] i_{cc} \quad [1.5]$$

$$\phi_{cc} = [M_{ccs}] \underline{i}_s + [M_{ccr}] \underline{i}_r + L_{cc} i_{cc} \quad [1.6]$$

where

$$[R_s] = \begin{pmatrix} R_{sa} & 0 & 0 \\ 0 & R_{sb} & 0 \\ 0 & 0 & R_{sc} \end{pmatrix} \quad [R_r] = \begin{pmatrix} R_{ra} & 0 & 0 \\ 0 & R_{rb} & 0 \\ 0 & 0 & R_{rc} \end{pmatrix}$$

$$[L_s] = \begin{pmatrix} L_{psa} + L_{f sa} & -\frac{L_{sab}}{2} & -\frac{L_{sac}}{2} \\ -\frac{L_{sab}}{2} & L_{psb} + L_{f sb} & -\frac{L_{sbc}}{2} \\ -\frac{L_{sac}}{2} & -\frac{L_{sbc}}{2} & L_{psc} + L_{f sc} \end{pmatrix}$$

$$[L_r] = \begin{pmatrix} L_{pra} + L_{fra} & -\frac{L_{rab}}{2} & -\frac{L_{rac}}{2} \\ -\frac{L_{rab}}{2} & L_{prb} + L_{frb} & -\frac{L_{rbc}}{2} \\ -\frac{L_{rac}}{2} & -\frac{L_{rbc}}{2} & L_{prc} + L_{frc} \end{pmatrix}$$

$$[M_{sr}] = \begin{pmatrix} M_{s_a r_a} \cos(\theta) & M_{s_a r_b} \cos(\theta + \frac{2\pi}{3}) & M_{s_a r_c} \cos(\theta - \frac{2\pi}{3}) \\ M_{s_b r_a} \cos(\theta - \frac{2\pi}{3}) & M_{s_b r_b} \cos(\theta) & M_{s_b r_c} \cos(\theta + \frac{2\pi}{3}) \\ M_{s_c r_a} \cos(\theta + \frac{2\pi}{3}) & M_{s_c r_b} \cos(\theta - \frac{2\pi}{3}) & M_{s_c r_c} \cos(\theta) \end{pmatrix}$$

$$[M_{rs}] = [M_{sr}]^T$$

$R_{sx}$  (resp.  $R_{ry}$ ) : proper resistance of stator phase (resp. rotor phase)

$L_{psx}$  et  $L_{fsx}$  : inductance and leakage stator inductance

$L_{psx} + L_{fsx}$  : proper inductance of stator phase

$L_{sxy}$  (resp.  $L_{rxy}$ ) : mutual inductance between two stator phases (resp. rotor phases)

$M_{s_x r_y}$  : mutual inductance between stator phase  $x$  and rotor phase  $y$

$M_{scc}$  (resp.  $M_{rcc}$ ) : mutual inductance between of stator phase (resp. rotor phase) and short-circuit winding

$\theta = p \cdot \theta_{\text{mechanical}}$  : electrical rotor angle

$p$  : number of pole-pairs

HYPOTHESIS. The previous electrical equations can be simplified with these usual hypothesis :

- symmetry and linearity of the electrical machine,
- both magnetomotive force in the airgap and the flux are sinusoidal,
- the magnetic circuit is not saturated and has a constant permeability,
- skin effect and core losses are neglected.

With these assumptions, we can write :

$$R_{sx} = R_s$$

$$R_{ry} = R_r$$

$$L_{psx} = L_{pry} = L_{sxy} = L_{rxy} = M_{s_x r_y} = L_p$$

In the previous electrical equations, the leakage are divided between stator and rotor phases. This method generate two coupled parameters  $L_{fsx}$  and  $L_{fsy}$ . One solution to simplify these equations is to globalize the leakage in the stator phase according to the relations:

$$L_{fry} = 0$$

$$L_{fsx} = L_f$$

[1.7]

The winding resistance are proportional to the number of inter turns, then the resistance  $R_{cc}$  of faulty winding  $B_{cc}$  can be written as :

$$R_{cc} = \eta_{cc} R_s$$

with

$$\eta_{cc} = \frac{n_{cc}}{n_s} = \frac{\text{Number of interturns short-circuit windings}}{\text{Total number of interturns in healthy phase}} \quad [1.8]$$

According to the previous hypothesis, the expressions of inductance and mutual inductances can be simplified :

$$\begin{aligned} L_{cc} &= \eta_{cc}^2 (L_p + L_f) \\ [M_{ccs}] &= \eta_{cc} L_p \begin{bmatrix} \cos(\theta_{cc}) & \cos(\theta_{cc} - \frac{2\pi}{3}) & \cos(\theta_{cc} + \frac{2\pi}{3}) \end{bmatrix} \\ [M_{ccr}] &= \eta_{cc} L_p \begin{bmatrix} \cos(\theta_{cc} - \theta) & \cos(\theta_{cc} - \theta - \frac{2\pi}{3}) & \cos(\theta_{cc} - \theta + \frac{2\pi}{3}) \end{bmatrix} \\ [M_{rcc}] &= [M_{ccr}]^T, \quad [M_{scc}] = [M_{ccs}]^T \end{aligned}$$

#### 1.2.1.2. Two-phases stator faulty induction model

To minimize the number of model variables, we use Concordia transformation which gives  $\alpha\beta$  values of same amplitude as  $abc$  ones. Thus, we define three to two axis transformation  $T_{23}$  as:

$$\begin{aligned} \underline{x}_{\alpha\beta s} &= T_{23} \underline{x}_s : \text{stator variables} \\ \underline{x}_{\alpha\beta r} &= P(\theta) T_{23} \underline{x}_r : \text{rotor variables} \end{aligned} \quad [1.9]$$

where  $\underline{x}_{\alpha\beta}$  is projection of  $\underline{x}$  following  $\alpha$  and  $\beta$  axis. Matrix transformations are defined as:

$$\begin{aligned} [T_{23}] &= \sqrt{\frac{2}{3}} \begin{bmatrix} \cos(0) & \cos(\frac{2\pi}{3}) & \cos(\frac{4\pi}{3}) \\ \sin(0) & \sin(\frac{2\pi}{3}) & \sin(\frac{4\pi}{3}) \end{bmatrix} \\ P(\theta) &= \begin{bmatrix} \cos(\theta) & \cos(\theta + \frac{\pi}{2}) \\ \sin(\theta) & \sin(\theta + \frac{\pi}{2}) \end{bmatrix} : \text{rotational matrix} \end{aligned}$$

The short circuit variables are localized on one axis, these projections on the two Concordia axis  $\alpha$  and  $\beta$  is defined as:

$$\underline{i}_{\alpha\beta cc} = \begin{bmatrix} \cos(\theta_{cc}) \\ \sin(\theta_{cc}) \end{bmatrix} \cdot i_{cc}, \quad \underline{\phi}_{\alpha\beta cc} = \begin{bmatrix} \cos(\theta_{cc}) \\ \sin(\theta_{cc}) \end{bmatrix} \cdot \phi_{cc} \quad [1.10]$$



Thus, equations (1.1-1.6) becomes:

$$\underline{U}_{\alpha\beta_s} = R_s \underline{i}_{\alpha\beta_s} + \frac{d}{dt} \underline{\phi}_{\alpha\beta_s} \quad [1.11]$$

$$\underline{0} = R_r \underline{i}_{\alpha\beta_r} + \frac{d}{dt} \underline{\phi}_{\alpha\beta_r} - \omega P \left( \frac{\pi}{2} \right) \underline{\phi}_{\alpha\beta_r} \quad [1.12]$$

$$\underline{0} = \eta_{cc} R_s \underline{i}_{\alpha\beta_{cc}} + \frac{d}{dt} \underline{\phi}_{\alpha\beta_{cc}} \quad [1.13]$$

$$\underline{\phi}_{\alpha\beta_s} = (L_m + L_f) \underline{i}_{\alpha\beta_s} + L_m \underline{i}_{\alpha\beta_r} + \sqrt{\frac{2}{3}} \eta_{cc} L_m \underline{i}_{\alpha\beta_{cc}} \quad [1.14]$$

$$\underline{\phi}_{\alpha\beta_r} = L_m (\underline{i}_{\alpha\beta_s} + \underline{i}_{\alpha\beta_r}) + \sqrt{\frac{2}{3}} \eta_{cc} L_m \underline{i}_{\alpha\beta_{cc}} \quad [1.15]$$

$$\begin{aligned} \underline{\phi}_{\alpha\beta_{cc}} = & \sqrt{\frac{2}{3}} \eta_{cc} L_m Q(\theta_{cc}) (\underline{i}_{\alpha\beta_s} + \underline{i}_{\alpha\beta_r}) \\ & + \left( \frac{2}{3} L_m + L_f \right) \eta_{cc}^2 Q(\theta_{cc}) \underline{i}_{\alpha\beta_{cc}} \end{aligned} \quad [1.16]$$

where

$\omega = \frac{d\theta}{dt}$  is rotor electrical pulsation

$L_m = \frac{3}{2} L_p$  : magnetizing inductance

$$Q(\theta_{cc}) = \begin{bmatrix} \cos(\theta_{cc})^2 & \cos(\theta_{cc}) \sin(\theta_{cc}) \\ \cos(\theta_{cc}) \sin(\theta_{cc}) & \sin(\theta_{cc})^2 \end{bmatrix}$$

If we neglect the leakage inductance  $L_f$  according to magnetizing inductance  $L_m$  in short circuit flux expressions (1.14-1.16), we can write new flux equations as:

$$\begin{cases} \underline{\phi}_{\alpha\beta_s} &= \underline{\phi}_{\alpha\beta_f} + \underline{\phi}_{\alpha\beta_m} \\ &= L_f \underline{i}_{\alpha\beta_s} + L_m (\underline{i}_{\alpha\beta_s} + \underline{i}_{\alpha\beta_r} - \tilde{\underline{i}}_{\alpha\beta_{cc}}) \\ \underline{\phi}_{\alpha\beta_r} &= \underline{\phi}_{\alpha\beta_m} = L_m (\underline{i}_{\alpha\beta_s} + \underline{i}_{\alpha\beta_r} - \tilde{\underline{i}}_{\alpha\beta_{cc}}) \\ \underline{\phi}_{\alpha\beta_{cc}} &= \eta_{cc} Q(\theta_{cc}) \underline{\phi}_{\alpha\beta_m} \end{cases} \quad [1.17]$$

where

$$\tilde{i}_{\alpha\beta_{cc}} = -\sqrt{\frac{2}{3}} \eta_{cc} \dot{i}_{\alpha\beta_{cc}}, \quad \tilde{\phi}_{\alpha\beta_{cc}} = \sqrt{\frac{3}{2}} \phi_{\alpha\beta_{cc}} \quad [1.18]$$

$\phi_{\alpha\beta_m}$ ,  $\phi_{\alpha\beta_f}$  are respectively magnetizing and leakage flux.

Then, short circuit current equation (1.13) becomes:

$$\tilde{i}_{\alpha\beta_{cc}} = \frac{2}{3} \frac{\eta_{cc}}{R_s} Q(\theta_{cc}) \frac{d}{dt} \phi_{\alpha\beta_m} \quad [1.19]$$

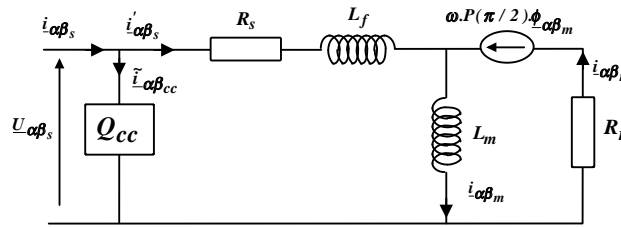


Figure 1.2. A short-circuit model of induction machine

According to this equation, the faulty winding  $B_{cc}$  becomes a simple unbalanced resistance element in parallel with magnetizing inductance. The existence of localization matrix  $Q(\theta_{cc})$  in equation [1.19] makes complex the state space representation in Concordia's axis. In a large range of industrial application, voltage drop in  $R_s$  and  $L_f$  is neglected according to stator voltage  $\underline{U}_{\alpha\beta_s}$  then, we can put a short circuit element  $Q_{cc}$  in input voltage border (Fig. 1.2). Line currents  $\dot{i}_{\alpha\beta_s}$  become the sum of short circuit current  $\tilde{i}_{\alpha\beta_{cc}}$  and usual current  $\dot{i}'_{\alpha\beta_s}$  in classical Concordia model.

It is much simpler to work in the rotor reference frame because we have only two stator variables to transform. Therefore, in state operation, all the variables have their pulsations equals to  $s\omega_s$  (where  $s$  is the slip and  $\omega_s$  is stator pulsation). We define Park's transformation as:

$$\underline{x}_{dq} = P(-\theta) \underline{x}_{\alpha\beta} \quad [1.20]$$

Afterward, the faulty model will be expressed under Park's reference frame. So, short circuit current [1.19] becomes:

$$\tilde{i}_{dq_{cc}} = \frac{2}{3} \frac{\eta_{cc}}{R_s} P(-\theta) Q(\theta_{cc}) P(\theta) \underline{U}_{dq_s} \quad [1.21]$$

### 1.2.1.3. Example of stator faulty model validation by spectral analysis

It is interesting to study the properties of current  $\tilde{i}_{dq_{cc}}$  in the short-circuit winding. In literature, it is shown that a spectral analysis of stator current allows to specify the nature of the defect [MOR 99b]. Indeed, a failure in the stator is reflected on the power spectral density by the appearance of spectrum lines around frequencies of  $2\omega$  whose origins can be explained in the following manner: The three phases stator currents create in the machine airgap a magnetic field turning at synchronous speed  $\omega_s = \frac{\omega}{1-g}$ . This magnetic field sweeps the rotor windings, which causes rotation of the motor. When the stator defect appears, it creates with the direct stator field an opposite field running at the speed  $-\omega_s$ . The stator currents are now direct and inverse following the imbalance of windings. The interaction of this field with that from the stator windings induce an electromagnetic forces at the frequency equal to  $2\omega_s$ .

Therefore, with Park's transformation, we can find in stator currents measurement an harmonic frequency at  $2\omega$ . For example, to validate a previous faulty model, it is necessary that the stator current in Park frame  $\underline{i}_{dq_s}$  presents a sinusoidal component around this frequency. We will use the additional short-circuit current term of  $\tilde{i}_{dq_{cc}}$  (Eq. 1.21) to justify the default model. For example, consider the case where a short circuit occurs on the first stator phase localized by the angle  $\theta_{cc} = 0$ . In this case, we can write:

$$Q(\theta_{cc}) = \begin{bmatrix} 1 & 0 \\ 0 & 0 \end{bmatrix}$$

The short-circuit current becomes:

$$\tilde{i}_{dq_{cc}} = R(\theta) \underline{U}_{dq_s} \quad [1.22]$$

with :

$$R(\theta) = \frac{2}{3} \frac{\eta_{cc}}{R_s} P(-\theta) Q(\theta_{cc}) P(\theta) = \frac{\eta_{cc}}{3 R_s} \begin{bmatrix} \cos(2\theta) + 1 & -\sin(2\theta) \\ -\sin(2\theta) & 1 - \cos(2\theta) \end{bmatrix}$$

The input voltages  $\underline{U}_{dq_s}$  is almost continuous in the Park frame, so they vary slowly compared to the terms of the matrix  $R(\theta)$  (except during the transient corresponding to a change of torque). The short-circuit current  $\tilde{i}_{d_{cc}}$  and  $\tilde{i}_{q_{cc}}$  are then a linear combinations of terms whose instantaneous pulsation at  $2\theta = 2\omega$ . These sinusoidal components at  $2\omega$  can be found in the measurement of stator currents  $\underline{i}_{dq_s}$ , explaining a possible stator imbalance.

For illustration, we present in the figure (1.3) a comparison between the power spectral density (Fourier Transform) of direct current Park  $i_{d_s}$  in healthy and faulty case (short-circuiting of 58 turns on phase  $a$ ). For a 1.1 kW induction machine, 4-poles, whose rotational speed is around 750 rpm (25 Hz), we measured the stator

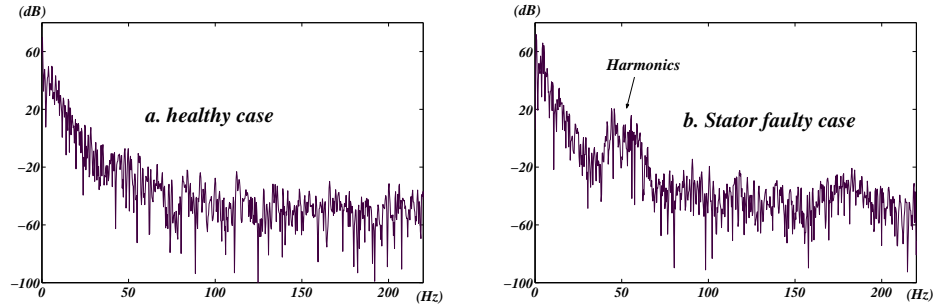


**Figure 1.3.** Power spectral density of stator current ( $f_s = 25 \text{ Hz}$ )

currents vector  $\underline{i}_s$  and performed the Park's transformation. Thus, we can observe on the figure (1.3) the appearance of additional spectrum lines in faulty case around  $2 \cdot f_s = 2 \cdot 25 \text{ Hz}$ .

#### 1.2.1.4. Global Stator faulty model

Fundamentally, we show that in faulty case, an induction machine can be characterized by two equivalent modes. The common mode model corresponds to the healthy dynamics of the machine (Park's model) whereas the differential one explains the faults. This model, very simple to implement because expressed in Park's frame, offers the advantage to explain the defect through a short circuit element dedicated to the faulty winding. On the other hand, it is unsuitable in case of simultaneous defects on several phases. Indeed, this representation is only adapted in case of single phase defect. In the presence of short circuits on several phases, this model translates the defect by aberrant parameters values, because it takes into account only a single winding.

To remedy it, we generalize this model by dedicating to each phase of the stator a short circuit element  $Q_{cc_k}$  to explain a possible faulty winding [BAC 01a][BAC 01b]. So, in presence of several short circuits, each faulty element allows the diagnosis of a phase by watching the value of the parameter. This simple deviation allows to indicate the presence of unbalance in the stator. The short-circuit current, noted  $\tilde{\underline{i}}_{dq_{cc_k}}$ , in  $k^{\text{th}}$  differential model can be expressed as:

$$\tilde{\underline{i}}_{dq_{cc_k}} = \frac{2}{3} \frac{\eta_{cc_k}}{R_s} P(-\theta) Q(\theta_{cc_k}) P(\theta) \underline{U}_{dq_s} \quad [1.23]$$

$Q(\theta_{cc_k})$  is the localization matrix (if the faults occurs on the phase a (resp. b and c) then the angle  $\theta_{cc_k}$  is equal to 0 rad (resp.  $\frac{2\pi}{3}$  and  $\frac{4\pi}{3}$ ).

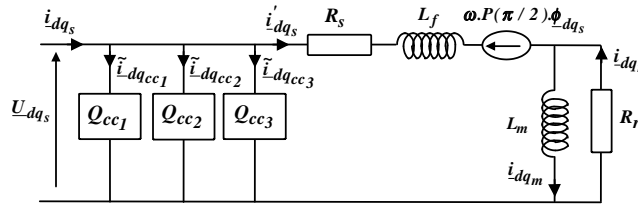


Figure 1.4. A global stator faulty model in  $dq$  frame

Figure (1.4) shows the global stator faulty model in  $dq$  Park's axis with global leakage referred to the stator.

### 1.2.2. Rotor faults modeling

As for stator fault, rotor fault is modeled by a new axis  $B_0$  referred to the first rotor axis  $a_r$  by the angle  $\theta_0$  [BAC 02]. This additional short circuited winding is at the origin of a stationary rotor field  $H_0(t)$  steered according to rotor fault axis (Fig. 1.5).

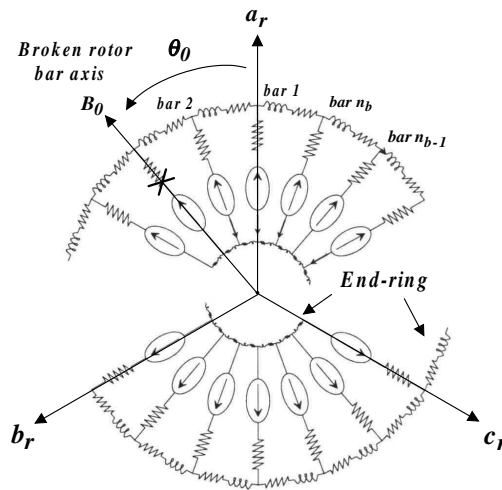


Figure 1.5. Broken rotor bar representation

Recently, rotor faults occurring in induction motors have been investigated. Various methods have been used, including measurement of rotor speed indicating speed

ripple, in the same way as spectral analysis of line current [FIL 94, INN 94, MAN 96]. The main problem concerning these monitoring methods is that they are essentially invasive, requiring obvious interruption of operation. Moreover, they are inappropriate under varying speed. For these reasons, parameter estimation is preferred for fault detection and diagnosis of induction motors [MOR 99b].

Parameter estimation is based on the simulation of a continuous state-space model of induction motor. This model assumes sinusoidal magnetomotive forces, non saturation of magnetic circuit and negligible skin effect. Under these assumptions, stator in  $dq$  Park's axis and squirrel cage rotor made of  $n_b$  bars can be modeled by an equivalent circuit.

So, two additional parameters are introduced in "differential" mode to explain rotor faults:

- The angle  $\theta_0$  between fault axis (broken rotor bar axis) and the first rotor phase. This parameter allows the localization of the broken rotor bar.
- To quantify the rotor fault, we introduce a parameter  $\eta_0$  equal to the ratio between the number of equivalent inter turns in defect and the total number of inter turns in one healthy phase:

$$\eta_0 = \frac{\text{Number of inter turns in defect}}{\text{Total number of inter turns in one phase}} \quad [1.24]$$

The number of turns in one rotor phase indeed fictitious. For  $n_b$  rotor bars, if we assume that the rotor cage can be replaced by a set of  $n_b$  mutually coupled loops, each loop is composed by two rotor bars and end ring portions [ABE 99, BAC 01a]; then the total number of rotor turns in one phase for three-phases representation is equal to  $\frac{n_b}{3}$ . For  $n_{bb}$  broken rotor bars, faulty parameter  $\eta_0$  becomes:

$$\eta_0 = \frac{3 n_{bb}}{n_b} \quad [1.25]$$

#### 1.2.2.1. Model of broken rotor bars

As stator faults modeling, we can write voltage and flux equations of new faulty winding  $B_0$  in  $dq$  Park's frame [BAC 02]:

$$0 = \eta_0 R_r i_o + \frac{d\phi_0}{dt} \quad [1.26]$$

$$\phi_0 = \frac{2}{3} \eta_0^2 L_m i_o + \sqrt{\frac{2}{3}} \eta_0 L_m [\cos(\theta_0) \quad \sin(\theta_0)] (\dot{i}_{dq_s} + \dot{i}_{dq_r}) \quad [1.27]$$

The current  $i_0$  in the faulty winding  $B_0$  creates a stationary magnetic field  $H_0$  being directed according to broken rotor bar axis. This additional magnetic field is at origin of faulty flux  $\phi_0$ . By throwing  $i_0$  and  $\phi_0$  on  $dq$  Park axis, one associates the stationary vectors:

$$\underline{i}_{dq_0} = \begin{bmatrix} \cos(\theta_0) \\ \sin(\theta_0) \end{bmatrix} i_0, \quad \underline{\phi}_{dq_0} = \begin{bmatrix} \cos(\theta_0) \\ \sin(\theta_0) \end{bmatrix} \phi_0$$

Equations [1.26] and [1.27] become relations between stationary vectors according to rotor frame. So, voltage and flux equations of stator, rotor and faulty winding of induction motor are given by:

$$\underline{U}_{dq_s} = R_s \underline{i}_{dq_s} + \frac{d}{dt} \underline{\phi}_{dq_s} + \omega P \left( \frac{\pi}{2} \right) \underline{\phi}_{dq_s} \quad [1.28]$$

$$\underline{\phi}_{dq_s} = L_f \underline{i}_{dq_s} + L_m (\underline{i}_{dq_s} + \underline{i}_{dq_r} + \sqrt{\frac{2}{3}} \eta_0 \underline{i}_{dq_0}) \quad [1.29]$$

$$\underline{0} = R_r \underline{i}_{dq_r} + \frac{d}{dt} \underline{\phi}_{dq_r} \quad [1.30]$$

$$\underline{\phi}_{dq_r} = L_m (\underline{i}_{dq_s} + \underline{i}_{dq_r}) + \sqrt{\frac{2}{3}} \eta_0 L_m \underline{i}_{dq_0} \quad [1.31]$$

$$0 = \eta_0 R_r \underline{i}_{dq_0} + \frac{d \underline{\phi}_{dq_0}}{dt} \quad [1.32]$$

$$\underline{\phi}_{dq_0} = \sqrt{\frac{2}{3}} \eta_0 L_m Q(\theta_0) (\underline{i}_{dq_s} + \underline{i}_{dq_r} + \sqrt{\frac{2}{3}} \eta_0 \underline{i}_{dq_0}) \quad [1.33]$$

By using same transformation as to obtain primary translation of an equivalent scheme in power transformer, we can write global flux equations as:

$$\begin{aligned} \underline{\phi}_{dq_s} &= \underline{\phi}_{dq_f} + \underline{\phi}_{dq_m} = L_f \underline{i}_{dq_s} + L_m (\underline{i}_{dq_s} + \underline{i}_{dq_r} - \tilde{\underline{i}}_{dq_0}) \\ \underline{\phi}_{dq_r} &= \underline{\phi}_{dq_m} = L_m (\underline{i}_{dq_s} + \underline{i}_{dq_r} - \tilde{\underline{i}}_{dq_0}) \\ \underline{\phi}_{dq_0} &= \eta_0 Q(\theta_0) \underline{\phi}_{dq_m} \end{aligned} \quad [1.34]$$

with

$$\tilde{\underline{i}}_{dq_0} = -\sqrt{\frac{2}{3}} \eta_0 \underline{i}_{dq_0}, \quad \tilde{\underline{\phi}}_{dq_0} = \sqrt{\frac{3}{2}} \underline{\phi}_{dq_0} \quad [1.35]$$

Also, current equation of faulty winding is given by:

$$\tilde{i}_{dq_0} = \frac{2}{3} \frac{\eta_0}{R_r} Q(\theta_0) \frac{d\phi_{dq_m}}{dt} = R_0^{-1} \frac{d\phi_{dq_m}}{dt} \quad [1.36]$$

where  $Q(\theta_0)$  is localization matrix.

#### 1.2.2.2. Equivalent electrical schemes

According to equation (1.36), faulty winding is a simple resistance element in parallel with magnetizing inductance and rotor resistance. Because, the reference frame is chosen according to rotor speed, it is impossible to translate this element in stator border  $\underline{U}_{dq_s}$ . Solution consists in establishing equivalent scheme of induction machine with adding Park's rotor resistance  $R_r$  to faulty one  $R_0$ . Thus, the equivalent resistance  $R_{eq}$  referred to the rotor is the stake in parallel with the rotor resistance and faulty resistance as:

$$\begin{aligned} R_{eq}^{-1} &= R_r^{-1} + R_0^{-1} \\ &= R_r^{-1} + \frac{2}{3} \eta_0 R_r^{-1} Q(\theta_0) \end{aligned} \quad [1.37]$$

By inversion, we obtain expression of an equivalent resistance matrix:

$$\begin{aligned} R_{eq} &= R_r + R_{\text{defect}} \\ &= R_r - \frac{\alpha}{1 + \alpha} Q(\theta_0) R_r \end{aligned} \quad [1.38]$$

with  $\alpha = \frac{2}{3}\eta_0$ .

Thus, equivalent rotor resistance in broken rotor bars case is a series connection of a healthy rotor resistance  $R_r$  and faulty resistance  $R_{\text{defect}}$ . Figure (1.6) is the resulting rotor fault circuit diagram in induction machines.

The angle  $\theta_0$  allows an absolute localization of the faulty winding according to the first rotor phase. Indeed, induced bars currents create a  $n_b$ -phases system and faulty angle  $\theta_0$  is fixed by initial rotor position according to stator position. On the other hand, when two broken rotor bars occur in machine, estimation of faulty angles  $\theta_{0_1}$  and  $\theta_{0_2}$  allows to obtain a gap angular  $\Delta\theta$  between broken bars [BAC 02]:

$$\Delta\theta = \theta_{0_2} - \theta_{0_1} \quad [1.39]$$



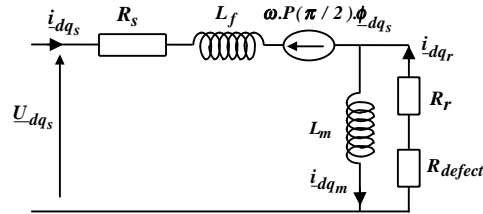


**Figure 1.6.** Broken rotor bars model

### 1.2.3. Global stator and rotor faulty model

In previous sections, two models of stator and rotor faults were presented. For a global simulation and detection of simultaneous stator and rotor faults, we propose the global faulty model including:

- Park's model with the electrical parameters ( $R_s$   $R_r$   $L_m$   $L_f$ )
- Stator faulty model with the three additional parameters ( $\eta_{cc_k}$ ,  $k = 1 - 3$ )
- Rotor faulty model with broken rotor bars parameters ( $\eta_0$ ,  $\theta_0$ )

Figure (1.7) shows a global electrical model of squirrel cage induction motors for stator and rotor faults detection.

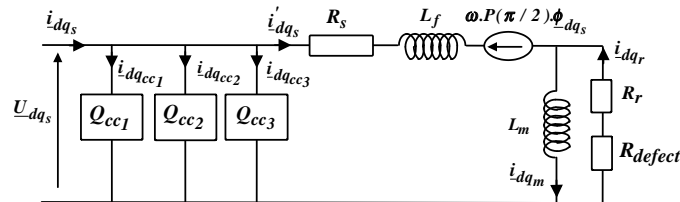


**Figure 1.7.** Stator and rotor faulty model of induction motors

#### 1.2.3.1. State space representation

For simulation and identification with the developed approach in chapter (7), it is necessary to write this faulty model in state space representation. If mechanical speed  $\omega$  is assumed to be quasi stationary with respect to the dynamics of the electric variables, the model becomes linear but not stationary with fourth order differential equations [BAC 01a]. For simplicity, the state vector is chosen composed of two-phases

components of the  $dq$  stator currents  $\underline{i}_{dq_s}$  and the rotor flux  $\underline{\phi}_{dq_r}$ . Then, the continuous time model of the faulty induction motor, expressed in the mechanical reference frame, is given by:

$$\dot{\underline{x}}(t) = A(\omega) \underline{x}(t) + B \underline{u}(t) \quad [1.40]$$

$$\underline{y}(t) = C \underline{x}(t) + D \underline{u}(t) \quad [1.41]$$

avec

$\underline{x} = [i_{d_s} \quad i_{q_s} \quad \phi_{d_r} \quad \phi_{q_r}]^T$  : state space vector

$\underline{u} = \begin{bmatrix} U_{d_s} \\ U_{q_s} \end{bmatrix}$ ,  $\underline{y} = \begin{bmatrix} i_{d_s} \\ i_{q_s} \end{bmatrix}$  : input and output vector

$$A(\omega) = \begin{bmatrix} -(R_s + R_{eq}) L_f^{-1} - \omega P(\pi/2) & (R_{eq} L_m^{-1} - \omega P(\pi/2)) L_f^{-1} \\ R_{eq} & -R_{eq} L_m^{-1} \end{bmatrix}$$

$$B = \begin{bmatrix} \frac{1}{L_f} & 0 \\ 0 & \frac{1}{L_f} \\ 0 & 0 \\ 0 & 0 \end{bmatrix}, C = \begin{bmatrix} 1 & 0 \\ 0 & 1 \\ 0 & 0 \\ 0 & 0 \end{bmatrix}^T, D = \sum_{k=1}^3 \frac{2\eta_{cc_k}}{3R_s} P(-\theta) Q(\theta_{cc_k}) P(\theta)$$

$$R_{eq} = R_r \cdot \left( I - \frac{\alpha}{1+\alpha} Q(\theta_0) \right)$$

### 1.2.3.2. Discrete time model

The discrete-time model is deduced from the continuous one by second order series expansion of the transition matrix [MOR 99b]. By using a second order series expansion and the mechanical reference frame, a sampling period  $T_e$  around 1 ms can be used. The usual first order series expansion (Euler approximation) requires very short sampling period to give a stable and accurate model. These approximation by series expansion are more precise with low frequency signals. Thus, discrete-time model is given by:

$$\underline{x}_{k+1} = \Phi_k \underline{x}_k + B_{d_k} \underline{u}_k \quad [1.42]$$

$$\underline{y}_k = C \underline{x}_k + D \underline{u}_k \quad [1.43]$$

where

$$\Phi_k = e^{AT_e} = I + A \frac{T_e}{1!} + A^2 \frac{T_e^2}{2!} \quad [1.44]$$

$$B_{d_k} = \left( I \cdot T_e + A \frac{T_e^2}{2 \cdot 1!} \right) B \quad [1.45]$$

and  $\underline{x}_k = \underline{x}(t_k)$  and  $\underline{y}_k = \underline{y}(t_k)$ . The components of the known input vector  $u_k$  are the average of the stator voltage between  $t_k$  and  $t_{k+1}$ .

### 1.3. Diagnosis procedure

Parameter estimation, presented in previous chapter, is the procedure that allows the determination of the mathematical representation of a real system from experimental data. Two classes of identification techniques can be used to estimate the parameters of continuous time systems: Equation Error and Output Error [LJU 87, MOR 99b]

– Equation Error techniques are based on the minimization of quadratic criterion by ordinary least-squares [LJU 87, TRI 88]. The advantage of these techniques is that they are simple and require few computations. However, there are severe drawbacks, especially for the identification of physical parameters, not acceptable in diagnosis, such as the bias caused by the output noise and the modeling errors.

– Output Error (OE) techniques are based on iterative minimization of an output error quadratic criterion by a Non Linear Programming (NLP) algorithm. These techniques require much more computation and do not converge to a unique optimum. But, OE methods present very attractive features, because the simulation of the output model is based only on the knowledge of the input, so the parameter estimates are unbiased [TRI 88, MOR 99b]. Moreover, OE methods can be used to identify non linear systems. For these advantages, the OE methods are more appropriate for diagnosis of induction motors [MOR 99b].

Parameter identification is based on the definition of a model. For the case of fault diagnosis in induction machines, we consider the previous mathematical model (Eqs. 1.40-1.41) and we define the parameter vector:

$$\underline{\theta} = [ R_s \quad R_r \quad L_m \quad L_f \quad \eta_{cc1} \quad \eta_{cc2} \quad \eta_{cc3} \quad \eta_0 \quad \theta_0 ]^T \quad [1.46]$$

As soon as a fault occurs, the machine is no longer electrically balanced. Using previous faulty modes, electrical parameters ( $R_s$ ,  $R_r$ ,  $L_m$  and  $L_f$ ) does not change and only the faulty parameters ( $\eta_{cc_k}$  and  $\eta_0$ ) vary to indicate a fault level according to relations:

Number of inter turns short windings at  $k^{\text{th}}$  phase :  $\hat{n}_{cc_k} = \hat{\eta}_{cc_k} \cdot n_s$

Number of broken bars :  $\hat{n}_{bb} = \frac{\hat{\eta}_0 n_b}{3}$

Thus, during industrial operation, diagnosis procedure by parameter estimation of induction machines requires sequential electrical data acquisitions. Using each set of

datas, identification algorithm computes a new set of electrical parameters to know the magnetic state of the machine and new faulty parameters to have an approximation of the number of inter turns short circuit windings and broken rotor bars.

### 1.3.1. Parameter estimation

Assume that we have measured  $K$  values of input-output  $(\underline{u}(t), \underline{y}^*(t))$  with  $t = k \cdot T_e$ , the identification problem is then to estimate the values of the parameters  $\underline{\theta}$ . Then, we define the output prediction error:

$$\underline{\varepsilon}_k = \underline{y}_k^* - \hat{\underline{y}}_k(\hat{\underline{\theta}}, \underline{u}) \quad [1.47]$$

where predicted output  $\hat{\underline{y}}_k$  is obtained by numerical simulation of the state space faulty model (Eq. 1.43) and  $\hat{\underline{\theta}}$  is an estimation of true parameter vector  $\underline{\theta}$ .

As a general rule, parameter estimation with OE technique is based on minimization of a quadratic criterion defined in the case of induction motor as :

$$J = \sum_{k=1}^K \underline{\varepsilon}_k^T \underline{\varepsilon}_k = \sum_{k=1}^K \left( (i_{ds_k}^* - \hat{i}_{ds_k})^2 + (i_{qs_k}^* - \hat{i}_{qs_k})^2 \right) \quad [1.48]$$

Usually, for induction motors, one has good knowledge on electrical induction motors parameters, so it is very interesting to introduce this information in the estimation process to provide more certainty on the uniqueness of the optimum. For this, we have applied the modification of the classical quadratic criterion [MOR 99b, TRI 88], in order to incorporate physical knowledge.

#### 1.3.1.1. Introduction of prior information

In order to incorporate physical knowledge or prior information, the classical quadratic criterion has been modified. The solution is to consider a compound criterion  $J_c$  mixing prior estimation  $\theta_0$  (weighted by its covariance matrix  $M_0$ ) and the classical criterion  $J$  (weighted by the variance of output noise  $\hat{\delta}^2$ ). Then, the compound criterion is usually defined as:

$$J_c = (\hat{\underline{\theta}} - \underline{\theta}_0)^T M_0^{-1} (\hat{\underline{\theta}} - \underline{\theta}_0) + \frac{\sum_{k=1}^K (\varepsilon_{ds_k}^2 + \varepsilon_{qs_k}^2)}{\hat{\delta}^2} \quad [1.49]$$

Thus, the optimal parameter vector minimizing  $J_c$  is the mean of prior knowledge and experimental estimation weighted by their respective covariance matrix.

In real case, we have no knowledge of the fault; indeed, no prior information is introduced on faulty parameter. Only electrical parameters ( $R_s$ ,  $R_r$ ,  $L_m$  and  $L_f$ ) are weighted in the compound criterion. Thus, covariance matrix is defined as:

$$M_0^{-1} = \text{diag} \left( \frac{1}{\sigma_{R_s}^2}, \frac{1}{\sigma_{R_r}^2}, \frac{1}{\sigma_{L_m}^2}, \frac{1}{\sigma_{L_f}^2}, 0, 0, 0, 0, 0 \right) \quad [1.50]$$

$\sigma_{R_s}^2$ ,  $\sigma_{R_r}^2$ ,  $\sigma_{L_m}^2$  and  $\sigma_{L_f}^2$  are respectively the variance of parameters with prior information  $R_s$ ,  $R_r$ ,  $L_m$  and  $L_f$ .

### 1.3.1.2. Nonlinear programming algorithm

We obtain the optimal values of  $\underline{\theta}$  by Non Linear Programming techniques. Practically, we use Marquardt's algorithm [MAR 63] for off-line estimation:

$$\hat{\underline{\theta}}_{i+1} = \hat{\underline{\theta}}_i - \{[J''_{\theta\theta} + \lambda \cdot I]^{-1} \cdot J'_{\theta}\}_{\hat{\underline{\theta}} = \hat{\underline{\theta}}_i} \quad [1.51]$$

with

$$J'_{c\theta} = 2 \cdot \left( M_0^{-1}(\hat{\underline{\theta}} - \underline{\theta}_0) - \frac{\sum_{k=1}^K \underline{\varepsilon}_k^T \cdot \underline{\sigma}_{k,\theta}}{\delta^2} \right) : \text{gradient.}$$

$$J''_{c\theta\theta} \approx 2 \cdot \left( M_0^{-1} + \frac{\sum_{k=1}^K \underline{\sigma}_{k,\theta} \cdot \underline{\sigma}_{k,\theta}^T}{\delta^2} \right) : \text{hessian.}$$

$\lambda$  : monitoring parameter.

$\underline{\sigma}_{k,\theta} = \frac{\partial \hat{y}}{\partial \underline{\theta}}$  : output sensitivity function.

### 1.3.1.3. Criterion weights designation

Prior information is mainly used to avoid aberrant estimates given by minimization of classical criterion. As a consequence, our interest is focused on the optimal choice of  $\underline{\theta}_0$ ,  $M_0$  and  $\hat{\delta}^2$ . Prior information can result from two origin:

- Experiments or motor information given by industrials. In this case,  $\theta_0$  and  $M_0$  are obtained by usual electrical tests performed on induction machines (locked rotor, load shedding, ...) and all material characteristics.

- Practically, prior information is given by physical knowledge and partial estimation. Firstly, a set of experiment and identification of only electrical parameters with classical criterion  $J$  is used in order to constitute an electrical reference value data base, their pseudo-covariance matrix  $M$  and the noise pseudo-variance are  $\hat{\delta}^2$  defined as:

$$M = \hat{\delta}^2 (\phi_d^T \phi_d + \phi_q^T \phi_q)^{-1} (\phi_d + \phi_q)^T (\phi_d + \phi_q) (\phi_d^T \phi_d + \phi_q^T \phi_q)^{-1} \quad [1.52]$$

$$\hat{\sigma}^2 = \frac{J_{opt}}{K - N} \quad [1.53]$$

where  $K$ ,  $N$  and  $J_{opt}$  are respectively the number of data, the number of parameters and the optimal value of experimental criterion. The matrix  $\phi_d$  and  $\phi_q$  are matrix of output sensitivity functions according to  $dq$  current axis.

Thus, the covariance matrix  $M_0$  is obtained by diagonal values of  $M$ . To evaluate the noise variance, it is necessary to use  $\hat{\delta}^2 > \hat{\sigma}^2$  to take into account the effect of modeling errors.

The motor used in the experimental investigation is a three phases, 1.1 kWatt, 4-poles squirrel cage induction machine (Fig. 1.8). The data acquisition was done at a sampling period equal to  $0.7 \text{ ms}$ . Before identification, measured variables are passed through a  $4^{th}$  order butterworth anti-aliasing filter whose cut-off frequency is  $500 \text{ Hz}$ .

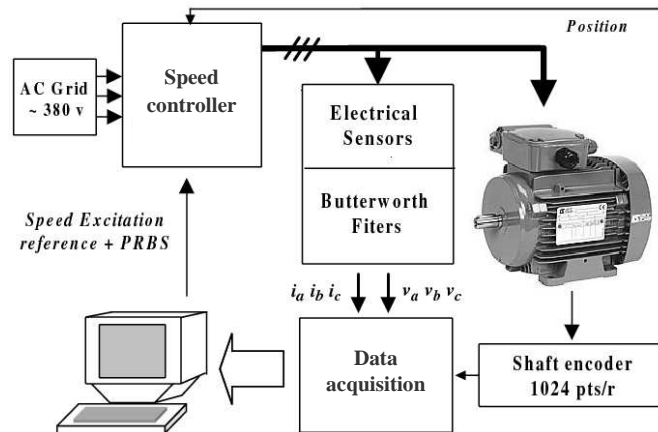


Figure 1.8. Motor experimental setup

With the mean of 10 realizations in healthy case, we obtained the reference of electrical parameters noted  $\underline{\theta}_{ref}$  and the weights of quadratic criterion. Then, for all experiments estimation, we used:

$$\underline{\theta}_{ref} = [ 9.81 \quad 3.83 \quad 0.436 \quad 7.62 \cdot 10^{-2} \quad 0 \quad 0 \quad 0 \quad 0 \quad \theta_{0_{init}} ]^T$$

$$M_0^{-1} = \text{diag}(5 \cdot 10^2, \quad 65 \cdot 10^2, \quad 17 \cdot 10^5, \quad 10^7, \quad 0, \quad 0, \quad 0, \quad 0, \quad 0)$$

The noise variance:  $\hat{\delta}^2 = 0.22$

### 1.3.2. Implementation

Experiments are performed en closed loop : The induction machine is driven by field oriented vector algorithm included in a speed control closed-loop and run under different loads with the help of a DC generator mechanically coupled to the motor. The speed excitation is realized with a Pseudo Random Binary Sequence (P.R.B.S) equal to 90 rpm added to the reference of the speed loop equal to 750 rpm. The mechanical position and the three phases voltages and currents are measured and translated in low frequencies by Park Transformation.

Stator windings were modified by addition of a number of tappings connected to the stator coils in the 1<sup>st</sup> and 2<sup>nd</sup> phases (464 turns by phase). These tappings correspond to 18 inter turns (3.88 %), 29 inter turns (6.25 %), 58 inter turns (12.5 %) and 116 inter turns (25 %). The other end of these external wires is connected to a terminal box, allowing introduction of shorted turns at several locations and levels in the stator winding. Different rotors, with broken bars, are used to simulate a bar breakage occurring during operation.

#### 1.3.2.1. Estimation results

Different tests (10 realizations by experiment) with inter turn short-circuit windings and broken rotor bars have been performed. Table 1.1 shows the mean of faulty parameter estimates for 10 acquisitions.

As observed in table 1.1, there is good agreement between a real fault and its estimation. All faulty parameters vary to indicate the values of inter turn short circuit in the three-stator windings and the number of broken rotor bars.

Experiments $n_{cc1}, n_{cc2}, n_{cc3}$ (inter turns), $n_{bb} (\Delta\theta)$	Estimation results (mean of 10 realizations)			
	$\hat{n}_{cc1}$	$\hat{n}_{cc2}$	$\hat{n}_{cc3}$	$\hat{n}_{bc}$
1) Healthy machine	5.57	3.52	-0.03	0.08
2) 18, 0, 0 (inter turns), 1 bar	17.86	-1.11	2.51	0.94
3) 0, 58, 0 (inter turns), 2 bars ( $\pi/2.8$ )	3.11	54.52	0.28	1.86
4) 18, 58, 0 (inter turns), 2 bars ( $2\pi/28$ )	16.05	53.31	-2.54	1.88
5) 58, 29, 0 (inter turns), 2 bars ( $\pi/2.8$ )	53.69	26.87	-2.46	1.82

**Table 1.1.** Estimation results of stator and rotor faults

Indeed, parametric approach gives good estimations of short circuit turns number  $\hat{n}_{cck}$ . The estimation error is negligible and does not exceed five turns in each situation

of defect. At simultaneous faults in several phases (case 4 and 5), we observe that the estimates of the faulty parameters of each phase is a realistic indication of the faults. This proves that each short circuit element explains the fault occurring at its phase and that no significant correlation exists between these elements. Moreover, broken rotor bars estimation  $\hat{n}_{bb}$  gives a satisfactory indication from the fault.

### 1.3.2.2. Parameters evolution

Figure (1.9) gives, for one realization in faulty situation (case 5), the evolution of electrical and faulty parameters during estimation procedure. For electrical state, It shows that their optimum values are achieved in only four iterations. On the other hand, their variation according to the initial values corresponding to prior information is negligible. For faulty state, it is shown that their variations, contrary from the electrical parameters, are very important. Each faulty parameters varies to indicate stator and rotor fault level occurring in the machine (example:  $n_{cc1}$  varies to approach the 58 inter turns in defect presents on the 1<sup>st</sup> phase and  $n_{bb}$  to approach 2 broken rotor bars).

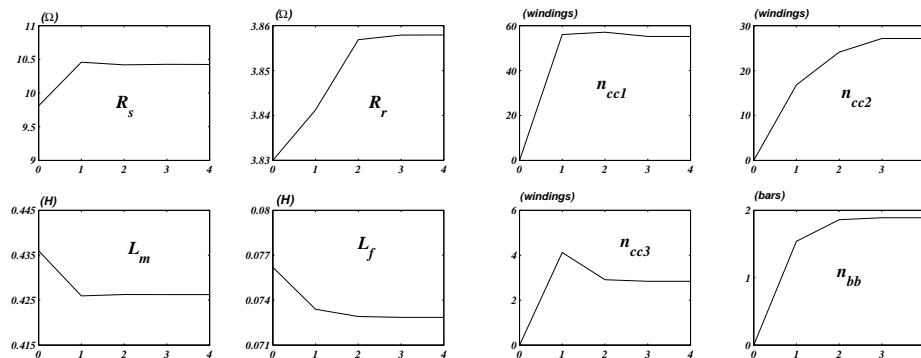
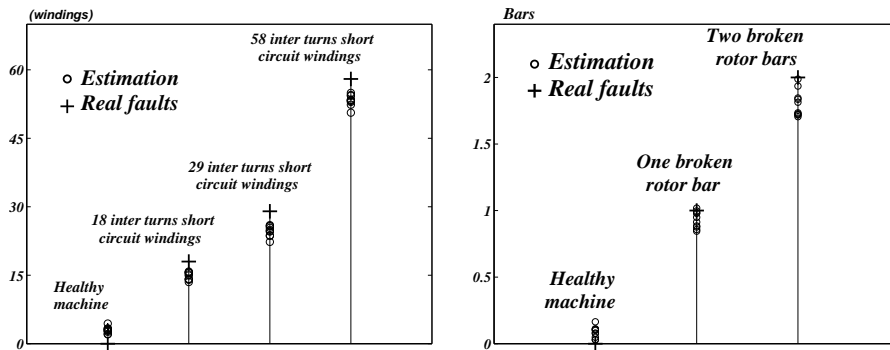


Figure 1.9. Estimation of electrical and faulty parameters at faulty case

This comparison is important because it is evident that only faulty parameters change when the faults occurs according to prior information principle. Moreover, electrical parameter variations are function of the temperature and of the magnetic state of the machine and are independent from the faults.

Figure (1.10) presents the evolution of inter turn short circuit estimation in one phase for several experiments and the dispersion of the 10 estimations in different situations of rotor faults. We observed that all the estimation results exhibit the good approximation of the stator and rotor faults.





**Figure 1.10.** Estimation of electrical and faulty parameters at stator and rotor faulty case

#### 1.4. Conclusion

The Output Error method associated with the compound criterion is a good tool for identification of continuous model parameters, and therefore very interesting for the diagnosis. In this chapter, we proposed thus a procedure for detection and localization of defects in the induction machine based on parameter estimation and on the use of a general faulty model.

Two faulty models, simple to implement, have been presented. The first one allows to explain a stator faults by three short-circuit elements, each element has been dedicated to a stator phase. A new equivalent Park's rotor resistance has been expressed to allow the decreasing of the number of rotor bars in faulty situation. Finally, the association of stator and rotor faulty element with the nominal model on induction machine allows to explain a simultaneous stator and rotor faults. This resulting model allows an extensive monitoring of the induction machine.

The proposed model has been validated on experimental test bench. The identification procedure has allowed on the one hand, the localization of stator faults at several phases and the determination of their number with a maximum error of six turns, and on the other hand, the quantification of the number of rotor broken bars. Thus, in situations of real defects, the diagnosis procedure by parameter estimation gives a very realistic indication of the imbalance occurring in the machine.

The monitoring methods based on parameter estimation has been poorly applied so far in diagnosis of physical systems, specially in electrical engineering: our experience shows that this method is well suitable for faults detection and localization. The association of parameter estimation technique with *a priori* information and faults modeling based on common and differential modes seems perfectly adapted to the case of the induction machine.

### 1.5. Bibliography

- [ABE 99] ABED A., BAGHLI L., RAZIK H., REZZOUG A., "Modelling induction motors for diagnosis purposes", *EPE'99*, Lausanne, Suisse, p. 1-8, September 1999.
- [BAC 01a] BACHIR S., TNANI S., POINOT T., TRIGEASSOU J. C., "Stator fault diagnosis in induction machines by parameter estimation", *IEEE International SDEMPED'01*, Grado, Italie, p. 235-239, September 2001.
- [BAC 01b] BACHIR S., TNANI S., TRIGEASSOU J. C., CHAMPENOIS G., "Diagnosis by parameter estimation of stator and rotor faults occurring in induction machines", *EPE'01*, Graz, Autriche, August 2001.
- [BAC 02] BACHIR S., Contribution au diagnostic de la machine asynchrone par estimation paramétrique, Ph.D. Thesis, Poitiers University, 2002.
- [BAC 06] BACHIR S., TNANI S., TRIGEASSOU J. C., CHAMPENOIS G., "Stator fault diagnosis in induction machines by parameter estimation", *IEEE Transactions on Industrial Electronics*, vol. 53, num. 3, p. 963-973, 2006.
- [FIL 94] FILLIPPITTI F., FRANCESHINI G., TASSONI C., VAS P., "Broken bar detection in induction machine : comparaison between current spectrum approach and parameter estimation approach", *IAS'94*, New York, USA, p. 94-102, 1994.
- [FRA 90] FRANK P. M., "Fault diagnosis in dynamical systems using analytical and knowledge based redundancy - A survey", *Automatica*, vol. 26, num. 3, p. 459-474, 1990.
- [GRE 97] GRELLET G., CLERC G., *Actionneurs électriques. Principes, modèles et commande*, Eyrolles, Paris, 1997.
- [INN 94] INNES A. G., LANGMAN R. A., "The detection of broken bars in variable speed induction motors drives", *ICEM'94*, December 1994.
- [LJU 87] LJUNG L., *System identification: Theory for the user*, Prentice Hall, USA, 1987.
- [LOR 93] LORON L., "Application of the extended Kalman filter to parameter estimation of induction motors", *EPE'93*, vol. 05, Brighton, p. 85-90, September 1993.
- [MAK 97] MAKKI A., AH-JACO A., YAHOUI H., GRELLET G., "Modelling of capacitor single-phase asynchronous motor under stator and rotor winding faults", *IEEE International SDEMPED'97*, Carry-le-Rouet, France, p. 191-197, September 1997.
- [MAL 99] MALÉRO M. G., ET AL, "Electromagnetic torque harmonics for on-line interturn shortcircuits detection in squirrel cage induction motors", *EPE'99*, Lausanne, Suisse, September 1999.
- [MAN 96] MANOLAS S. T., TEGOPOULOS J., PAPADOPOULOS M., "Analysis of squirrel cage induction motors with broken rotor bars", *ICEM'96*, Vigo, Espagne, p. 19-23, 1996.
- [MAR 63] MARQUARDT D., "An Algorithm for least-squares estimation of non-linear parameters", *Soc. Indust. Appl. Math*, vol. 11, num. 2, p. 431-441, 1963.
- [MEN 99] MENSLER M., Analyse et étude comparative de méthodes d'identification des systèmes à représentation continue. Développement d'une boîte à outil logicielle, Ph.D. Thesis, Nancy I University, 1999.

- [MOR 99a] MOREAU S., TRIGEASSOU J. C., CHAMPENOIS G., GAUBERT J. P., "Diagnosis of Induction Machines: A procedure for electrical fault detection and localization", *IEEE International SDEMPED'99*, Gijon, Spain, p. 225-230, September 1999.
- [MOR 99b] MOREAU S., Contribution à la modélisation et à l'estimation paramétrique des machines électriques à courant alternatif: Application au diagnostic, Ph.D. Thesis, Poitiers University, 1999.
- [SCH 99] SCHAEFFER E., Diagnostic des machines asynchrones: modèles et outils paramétriques dédiés à la simulation et à la détection de défauts, Ph.D. Thesis, Nantes University, 1999.
- [TRI 88] TRIGEASSOU J. C., *Recherche de modèles expérimentaux assistée par ordinateur*, Technique et Documentation Lavoisier, Paris, 1988.
- [TRI 99] TRIGEASSOU J. C., GAUBERT J. P., MOREAU S., POINOT T., "Modélisation et identification en génie électrique à partir de résultats expérimentaux", *Journées 3EI'99*, Supelec Gif-sur-Yvette, March 1999.
- [VAS 94] VAS P., FILIPPETTI F., FRANCESCHILI G., TASSONI C., "Transient modelling oriented to diagnostics of induction machines with rotor asymmetries", *ICEM'94*, December 1994.

## Chapter 2

### Index

Diagnosis, 263  
Marquardt's algorithm, 265  
Output error technique, 264  
Prior information, 264

Rotor faulty model, 257  
Spectral analysis, 255  
Stator and rotor faulty model, 261  
Stator faulty model, 249